Air Quality, Atmosphere & Health
https://doi.org/10.1007/s11869-025-01749-w

Multi-routine-data driven spatio-temporal short-term predictions for surface ozone in China

Canju Zheng[1,5] · Hengqing Shen[2] · Jianan Sun[3] · Guangliang Liu[1,5] · Haowei Cao[1,5] · Jie Zhang[1,5] · Xiang Gong[4,6] · Da Xu[1,5]

Received: 5 December 2024 / Accepted: 6 May 2025

Abstract

Ozone (O_3) is a major atmospheric pollutant, and accurate prediction of its concentrations remains challenging due to its complex nonlinear relationships with precursor compounds. Existing machine learning methods have mainly focused on single-site or spatial predictions, lacking research on spatio-temporal short-term predictions based on simple factors. To address this gap, the MRD-O_3former, a deep learning model driven by multi-routine data, was developed to predict short-term hourly spatio–temporal surface ozone concentrations over China. The model exhibits strong spatio–temporal consistency, achieving a high correlation coefficient ($r^2 = 0.85 \sim 0.90$) and low normalized mean biases (NMBs) between -15% and 15% at the national scale compared to reanalysis ozone data. Both ablation experiments and permutation importance analysis reveal that historical ozone levels play a primary role in next-day ozone prediction, while meteorological factors such as wind speed and temperature also make significant contributions. Regional validation confirms the model's effectiveness in the Beijing-Tianjin-Hebei region. Moreover, the study investigates the differential impact of crucial factors in urban and rural areas, revealing that historical ozone levels and meteorological factors significantly influence rural areas. However, the influence of historical ozone levels on urban ozone prediction is relatively small, especially during the summer. This suggests that urban ozone undergoes rapid formation and removal processes. These findings highlight the promising potential of deep learning techniques in accurately predicting spatiotemporal short-term ozone concentrations and interpreting the mechanism and source for ozone pollution.

Keywords Multi-factor · Data-driven · Ozone concentration · Spatio-temporal prediction

Introduction

Ozone (O_3) is a secondary pollutant formed by complex chemical reactions involving nitrogen oxides (NO_x) and volatile organic compounds (VOCs) (Shu et al. 2023). In the clean atmosphere, a photochemical equilibrium is established among NO, NO_2, and O_3 (reactions 1–3).

$$NO_2 + h\nu(< 420nm) \rightarrow NO_2^* \rightarrow NO + O \quad (1)$$

$$O + O_2 + M \rightarrow O_3 + M \quad (2)$$

$$NO + O_3 \rightarrow NO_2 + O_2 \quad (3)$$

Once biogenic or anthropogenic VOCs are emitted into the atmosphere, they undergo oxidation processes that result in the formation of HO_2 and RO_2 radicals, which react with NO:

Canju Zheng and Hengqing Shen contributed equally to this work.

✉ Guangliang Liu
guangliangliu@163.com

1 Key Laboratory of Computing Power Network and Information Security, Ministry of Education, Shandong Computer Science Center, Qilu University of Technology (Shandong Academy of Sciences), Jinan, China

2 Environment Research Institute, Shandong University, Qingdao 266237, Shandong, China

3 Ningbo Yonghuanyuan Environmental Engineering and Technology Co., LTD, Ningbo 315012, Zhejiang, China

4 School of Mathematics and Physics, Qingdao University of Science and Technology, Qingdao 266061, China

5 Shandong Provincial Key Laboratory of Computer Networks, Shandong Fundamental Research Center for Computer Science, Jinan, China

6 Qingdao Innovation Center of Artificial Intelligence Ocean Technology, Qingdao 266061, China

Published online: 14 May 2025

$$RO_2 + NO \rightarrow NO_2 + RO \quad (4)$$

$$HO_2 + NO \rightarrow NO_2 + OH \quad (5)$$

The above two reactions trigger the conversion of NO to NO_2 and accumulate O_3 in the atmosphere (Yang and Zhao 2023).

High concentrations of near-surface O_3 have detrimental effects on vegetation and pose risks to human respiratory, nervous, and immune systems (Gong et al. 2021; Yu et al. 2021). Despite significant improvements in reducing particulate matter ($PM_{2.5}$), implementing air pollution control measures in China has seen a rise in surface ozone pollution in recent years (Liu et al. 2023). From 2013 to 2018, China experienced a significant increase in the average annual O_3 concentration, with an increase rate of 1.84 μg m^{-3} $year^{-1}$. This notable increase was primarily observed in the eastern, central, and northern regions of China (He et al. 2023). The phenomenon of increased ozone concentrations, despite intensified control efforts, suggests that our understanding of the ozone formation mechanism is still incomplete. This highlights the need for a more comprehensive understanding of the factors influencing ozone formation to predict and address ozone pollution accurately.

Numerical models are commonly used to estimate air pollutant concentrations, including O_3, based on physical and chemical processes. However, due to inherent errors in the numerical models, inaccuracies in the input data, and simplified chemical mechanisms, O_3 predictions are often biased from observations (Xiong et al. 2023). Studies have shown serious biases in simulating O_3 concentrations, particularly during periods of high concentrations (Sayeed et al. 2022). Different models showed varying biases, with GEOS-Chem and CAMx generally overestimating ambient ozone concentrations, while the biases of CMAQ, WRF-Chem, and NAQPMS were less certain (Yang and Zhao 2023). The limited coverage of ozone monitoring stations, particularly in remote regions, hinders accurate and comprehensive spatio-temporal distribution assessment of ozone concentrations (Mu et al. 2023a). The formation of O3 is influenced by various drivers, including precursor emissions, chemical processes, and meteorology (Xu et al. 2023). Numerically driven models offer logical reasoning and explanatory capabilities but face challenges in obtaining high-resolution emission inventories and high computational costs, limiting their accuracy and efficiency (Mu et al. 2023b).

Data-driven approaches offer advantages over physical models as they can learn the relationships between pollutants and environmental variables from multivariate data through machine-learning or deep-learning algorithms (Pan et al. 2023). Deep learning models in the field of O_3 concentration prediction are mainly divided into three categories: one is using temporal modeling, the usual practice is to consider the O_3 data as a one-dimensional time series, and the main models include RNN, LSTM, GRU,1D CNN and so on. For example, Hong et al. (2023) used multi-order difference embedded LSTM (MDELSTM). Through statistical analysis of the O_3 time series, the multi-order difference module is flexibly embedded into an LSTM-based deep learning prediction model to perform hourly prediction on the O_3 concentration. The second category models spatio–temporal and incorporates spatial information into deep learning models to improve prediction accuracy. This is mainly achieved by integrating spatio-temporal network architectures such as CNN, LSTM, and GNN. For example, Pak et al. (2018) proposed a CNN-LSTM hybrid model that combines a convolutional neural network (CNN) and a long-short-term memory network (LSTM) to predict the 8-h average O_3 concentration of the following day in Beijing, China. Wu et al. (2023) proposed a deep learning-based Res-GCN-BiLSTM hybrid model that combines a residual neural network (ResNet), a graphical convolutional network (GCN), and a bidirectional long-term memory (BiLSTM) for predicting short-term regional NO_2 and O_3 concentrations. The results show that the above hybrid structure model can utilize the advantages of each module for the improvement of the prediction accuracy. The third type of deep learning model is the Transformer architecture, which is based on the attention mechanism, and such models overcome the limitations of traditional neural networks, such as memory constraints induced by parallel training of samples and processing of long-term sequences. Liang et al. (2023) proposed a variant of the transformer called AirFormer for predicting China's nationwide air quality, covering thousands of locations with unprecedented fine spatial granularity. Most existing deep learning models typically have a large number of network parameters, resulting in high computational complexity. Coupled with the time-sensitivity of O_3 prediction, fast and accurate prediction is required. Therefore, how to effectively reduce the computational complexity of deep learning models is one of the key issues in current research (Zhang et al. 2024).

Recently, Gao et al. (2022a) proposed the Earthformer model, which is a hierarchical Transformer codec model based on the Cuboid Attention Block. Its Cuboid Attention Block contains mechanism patterns such as Axial Attention, Video SwinTransformer, Segmented Spatio-Temporal Attention, etc., which can internally distribute and collect the key information of global observation data and solve the high complexity of Transformer architecture in obtaining high-dimensional spatio-temporal observation data applications. The formation of O_3 involves a variety of drivers, and there is a complex nonlinear relationship between the drivers. Therefore, Earthformer has potential advantages in the field of O_3 prediction. In addition to the significant influence of

meteorological factors on O_3, human activities are closely related to O_3, e.g., the Urban–Rural Disparities and traffic data have been identified as variables that influence air quality prediction results (Ganji et al. 2020; Wen et al. 2022). Therefore, studying the effects of urban and rural data, energy structure, transportation data, and other factors on O_3 could provide valuable suggestions for its prediction.

The study introduces the MRD-O_3former model, a deep-learning approach for short-term hourly surface O_3 prediction in China. By incorporating a multi-channel Earthformer architecture and utilizing multi-routine data from the previous 24 h, the model aims to provide fast and accurate forecasts. Ablation experiments and permutation importance analysis were conducted to assess the importance of different factors in ozone prediction. The model's performance was evaluated in the Beijing-Tianjin-Hebei region, examining its effectiveness in capturing localized ozone patterns. Additionally, the study investigated the contributions of drivers to ozone concentrations in urban and rural areas separately using permutation importance analysis. These efforts collectively contribute to improving ozone understanding and prediction capabilities.

Methodology

Study areas and data

The study encompassed the entire region of China, considering the complex factors that influence O_3 concentrations. To explore the spatial and temporal variability of O_3, a diverse dataset incorporating multiple types of data was compiled, and detailed information is provided in Table S1. The dataset comprised six years, from January 1, 2013, to December 31, 2018. These datasets were divided into a training set (2013–2016), a validation set (2017), and a test set (2018).

The datasets can be categorized into two main categories:

(1) Conventional air pollutants: NO_x and VOCs are the main precursors of O_3. However, due to limitations in the data availability and monitoring system for VOCs, conventional routine pollutants were used instead. The selected conventional air pollutant factors include O_3, $PM_{2.5}$, PM_{10}, SO_2, NO_2, and CO. These data were obtained from the China Air Quality Reanalysis Dataset (CAQRA) (https://doi.org/10.11922/sciencedb.00053, last access: 10 April 2024). Using these conventional pollutants, the study aims to replace ozone precursors and reduce the reliance on additional ozone monitoring stations.

(2) Meteorological data: The study incorporates meteorological factors such as wind speed (u and v), pressure, relative humidity, temperature, and solar ultraviolet radiation (UVB). Wind speed data (u, v), pressure, relative humidity, and temperature are obtained from the China Air Quality Reanalysis Dataset (CAQRA), while solar ultraviolet radiation (UVB) data is sourced from the European Centre for Medium-Range Weather Forecasts (ECMWF) European Reanalysis Dataset Generation 5 (ERA5) (https://cds.climate.copernicus.eu/cdsapp#!/dataset/, last access: 10 April 2024). These meteorological factors are included to capture the influence of weather conditions on ozone concentrations.

All the mentioned drivers in the study are interpolated uniformly to a spatial resolution of 15 km × 15 km and a temporal resolution of 1 h using cubic spline interpolation. The resulting dataset encompasses a total of 43,824 h. Spatially, it is represented by a 320 × 432 data matrix. The dataset consists of 12 different types of data, including $PM_{2.5}$, PM_{10}, SO_2, NO_2, CO, O_3, wind speed (u, v), pressure, solar ultraviolet radiation (UVB), relative humidity, and temperature.

MRD-O_3former

The MRD-O_3former model is developed based on the Earthformer, a space–time Transformer for Earth system forecasting (Gao et al. 2022b). The Earthformer model utilizes a hierarchical transformer encoder-decoder architecture with cuboid attention. Fig S1 illustrates the steps involved in the cuboid attention layer: "decompose", "attend", and "merge". In the decomposition step, the input spatio-temporal tensor is divided into non-overlapping rectangles using either a local or expansive decomposition strategy. Self-attention is then applied within each cuboid attention layer, allowing elements within a cuboid to focus on both local elements and global vectors. This enables local cuboids to capture the overall system dynamics and share information with each other. After the attention step, the resulting sequence of rectangles is merged back into the original input shape to obtain the final output of cuboid attention.

The MRD-O_3former model is shown in Fig. S1. It takes 12 types of input data, including $PM_{2.5}$, PM_{10}, SO_2, NO_2, CO, O_3, wind speed (u, v), pressure (psfc), relative humidity (RH), temperature (temp), and solar ultraviolet radiation (UVB) for the first 24 h. The model then generates predictions for the next 24 h of O_3. The Earthformer model parameters used in training are described in Table S2. The model produces non-autoregressive predictions, which can be represented by the mathematical equation:

$$\hat{O}_{t+24} \cdots \hat{O}_{t+1} = F\left(O_t \cdots O_{t-23}\right) \tag{6}$$

Here, t represents the current time, F denotes the ozone prediction model, and O_t···O_(t-23) represents the input data for the past 24 h.

Evaluation indicators

The performance of the model was evaluated using statistical metrics, including coefficient of determination (r^2), Mean Absolute Error (MAE), Root Mean Square Error (RMSE), and Normalized Mean Bias (NMB), as described in Eqs. (7) - (10).

The coefficient of determination (r^2) measured the linear correlation between forecasts and reanalyzed data. MAE assessed the closeness between predictions and observations, while RMSE quantified the dispersion between predicted and observed values.

$$r^2 = 1 - \frac{\sum_{i=1}^{n}\left(y_i - \hat{y}\right)^2}{\sum_{i=1}^{n}\left(y_i - \bar{y}\right)^2} \tag{7}$$

$$MAE = \frac{1}{n}\sum_{i=1}^{n}\left|\hat{y}_i - y_i\right| \tag{8}$$

$$RMSE = \sqrt{\frac{1}{n}\sum_{i=1}^{n}\left(\hat{y}_i - y_i\right)^2} \tag{9}$$

$$NMB = \frac{\sum_{i=1}^{n}(\hat{y}_i - y_i)}{\sum_{i=1}^{n}(y_i)} \times 100 \tag{10}$$

where y_i is the true value of O_3; $\bar{y}$ is the average of the true value; $\hat{y}_i$ represents the predicted value; n is the number of samples.

Permutation importance

Permutation Importance (PI) is a method used to estimate the importance of variables in a trained model (Huang et al. 2023). It quantifies the contribution of a feature (x_j) to the model's performance on a target variable (y) by randomly permuting the values of feature x_j in the input data and measuring the resulting decrease in performance compared to the original data. The larger the decrease in performance, the more important the feature is considered to be. PI was initially introduced for Random Forests (RF) and has since gained popularity. The formula for PI is:

$$PI_j = \mathrm{loss}(\hat{f}(x_j^*), y) - l(\hat{f}(x), y) \tag{11}$$

where x_j^* is created by permutation of the values in the j-th feature, x is the un-permuted input feature matrix, y is the observation dataset, $\hat{f}$ is the prediction function, and loss is the error function that uses the values of RMSE.

Results and discussion

Spatiotemporal distribution of the predicted O_3 concentration

Our model accurately predicted ozone concentrations across China for each season in 2018, as indicated by the reasonable agreement with the reanalysis data (Fig. 1). Ozone exhibited high spatial and temporal heterogeneity throughout the year. In spring and summer, ozone concentrations were higher compared to autumn and winter (0–100 μg m^{-3}), especially in the northern regions of China. This can be attributed to stronger photochemical

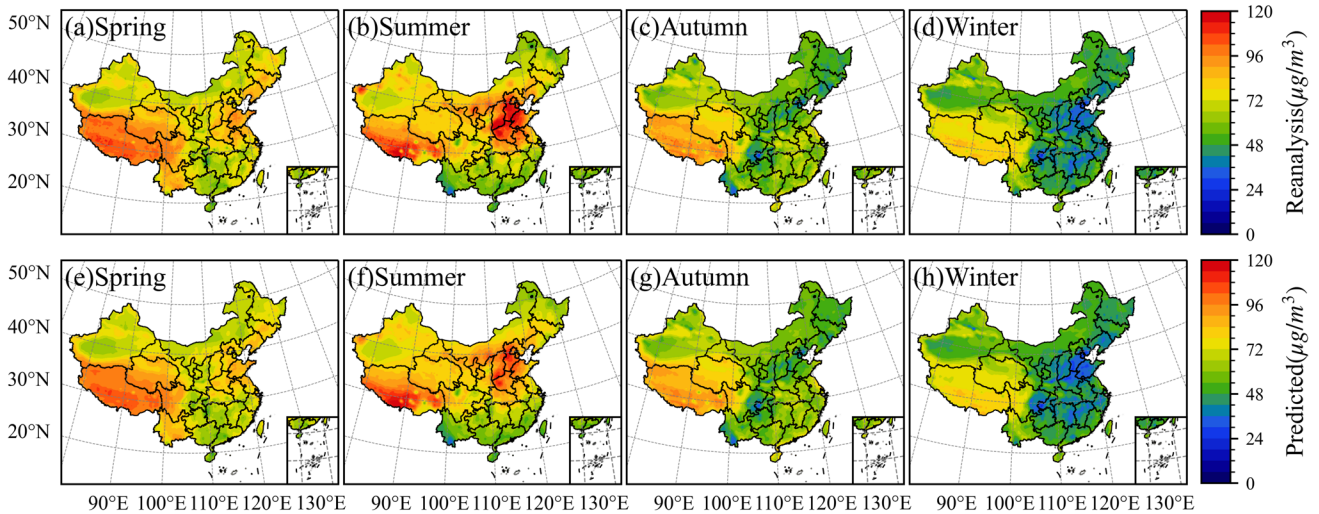

Fig. 1 Spatial distribution of reanalyzed (**a**-**d**) and predicted (**e**–**h**) O_3 concentrations for different seasons in 2018

reactions in the north during spring and summer, as well as the ozone titration effect caused by high concentrations of NO during winter (Yang et al. 2019). It is worth noting that the Qinghai-Tibet Plateau had relatively high ozone concentrations throughout the year despite having low ozone precursor concentrations. The high ozone levels in the plateau region, especially in spring and summer, are primarily due to the strong downward transport of high concentrations of ozone from the upper atmosphere caused by enhanced convection (Yin et al. 2023). The highest ozone concentrations in southern China occur during autumn, which can be attributed to the unfavorable conditions for photochemical reactions during the summer monsoon season (Li et al. 2018). The spatial and temporal heterogeneity indicates noticeable differences in ozone formation mechanisms among different regions, with simulations based on chemical mechanism models possibly having significant deviations (Mu et al. 2023b). Machine learning-based methods developed by this study can effectively capture the spatiotemporal variations of ozone in China.

Evaluations of model performance

In terms of overall national average performance, the model demonstrates a good simulation of ozone concentrations nationwide (Fig. S2). The coefficients of determination and normalized mean biases (NMBs) obtained for each season range from 0.85 to 0.90 and −0.43% to −0.26%, respectively. Even when considering the spatial distribution, the model's simulation of ozone concentrations remains relatively accurate. The NMB ranges from −15% to 15%, with slight underestimation observed in the summer in the North China Plain and overestimation in the autumn in the North China Plain and South China (Fig. 2). Regarding other evaluation parameters, the regions with larger prediction deviations are mainly concentrated in the summer in the North China Plain (average MAE = 6.56 μg m^{-3}, RMSE = 10.69 μg m^{-3}), while the best predictions are observed in the winter (MAE = 4.69 μg m^{-3}, RMSE = 7.07 μg m^{-3}). Spatially, the MAE is concentrated within 15 μg m^{-3}, and the RMSE within 20 μg m^{-3} in most parts of the country. The overestimation or underestimation of ozone concentrations is primarily observed in

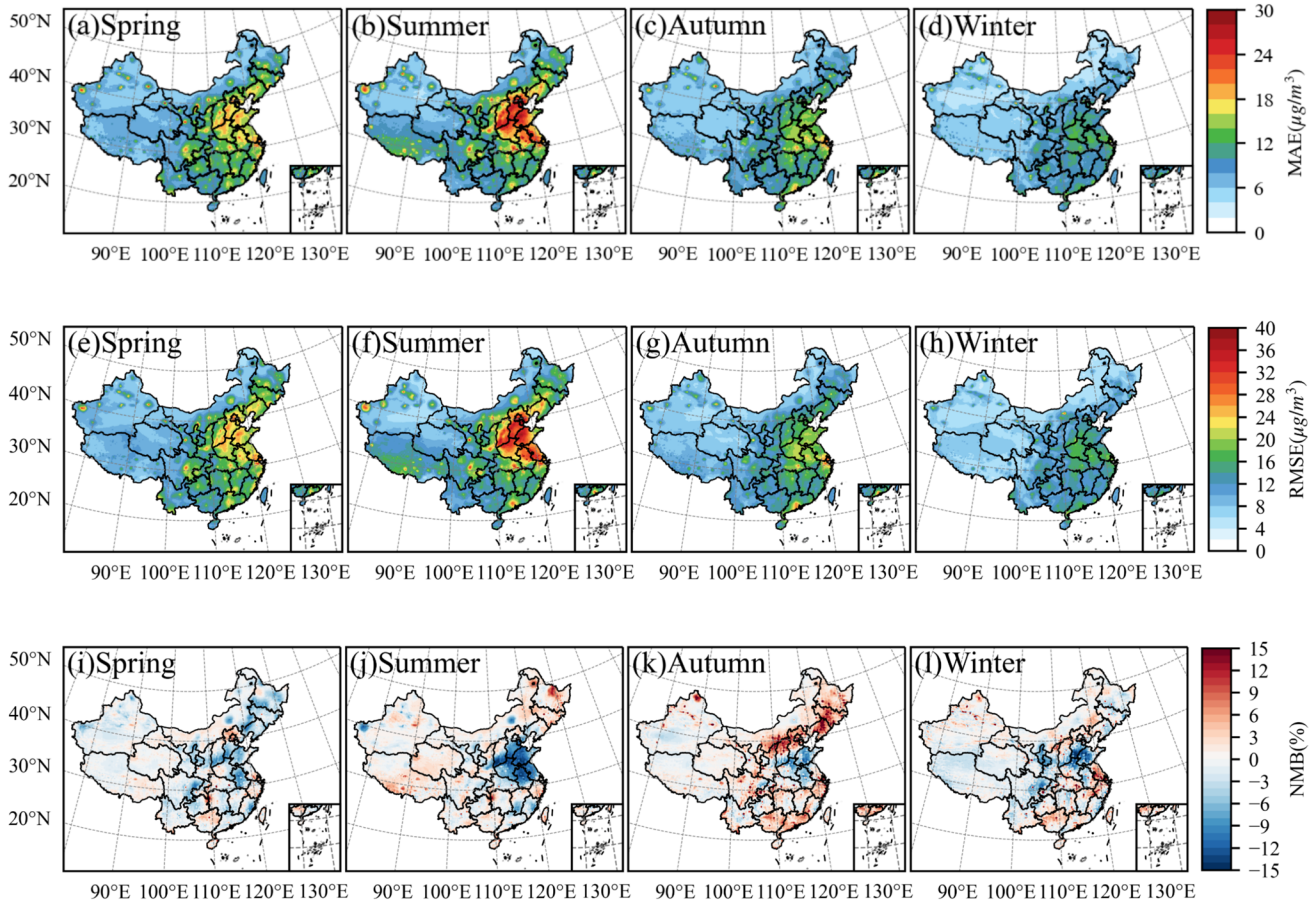

Fig. 2 Spatial distribution of temporally-averaged MAE (**a**-**d**), RMSE (**e**–**h**), and NMB (**i**-**l**) across seasons between reanalysis and predicted O_3 concentrations

the Beijing-Tianjin-Hebei region. These discrepancies may be attributed to the region's high anthropogenic precursor emissions, leading to complex ozone formation pathways. Similar findings were reported by (Cheng et al. 2022). In conclusion, the MRD-O_3former model performs well across all four seasons when considering the overall performance and evaluation metrics.

Quantification of critical drivers for O_3 prediction

We conducted factor ablation experiments and PI analysis to assess the specific contributions of various factors to surface O_3 prediction. The factors considered included $PM_{2.5}$, PM_{10}, SO_2, NO_2, CO, O_3, wind speed (u, v), pressure (psfc), relative humidity (RH), temperature (temp), and solar ultraviolet radiation (UVB).

Figure 3 illustrates the differences in MAE and RMSE after the ablation of different variables in spring, summer, autumn, and winter. The ablation experiments aim to determine the contribution of a factor by removing it, and then analyzing the resulting ozone prediction performance. Historical O_3 concentrations had the most significant effect on O_3 concentrations, followed by wind speed (u, v), temperature, pressure, relative humidity, solar UV radiation, and conventional air pollutants. Removal of historical O_3 significantly increased MAE and RMSE in all seasons. Specifically, the MAE and RMSE would increase by 22.37 μg m^{-3} and 25.92 μg m^{-3} in spring, 16.87 μg m^{-3} and 21.05 μg m^{-3} in summer, 19.00 μg m^{-3} and 23.33 μg m^{-3} in autumn, and 16.38 μg m^{-3} and 21.25 μg m^{-3} in winter, respectively. Wind velocity (u, v) is the second most influential factor, and its absence also leads to an increase in MAE and RMSE in all seasons. The mean MAE and RMSE increase by 11.04 μg m^{-3} and 12.70 μg m^{-3} in spring, 13.43 μg m^{-3} and 14.60 μg m^{-3} in summer, 12.02 μg m^{-3} and 13.57 μg m^{-3} in autumn and 13.73 μg m^{-3} and 15.74 μg m^{-3} in winter, respectively. Among the meteorological factors, wind speed (u,v) had a more significant effect on surface O_3 concentration, a finding consistent with a previous study (Wang et al. 2017), which showed that wind speed (u,v) affects ozone concentration by diluting ozone and transporting ozone precursors. Similarly, pressure affects ground-level O_3 concentrations mainly by influencing other meteorological elements (especially wind speed and direction) (Chen et al. 2020). The results show that temperature and humidity are second only to wind speed (u,v) for O_3 prediction and that temperature is the most important meteorological factor in all seasons except winter, where it is no longer the dominant factor due to lower temperature (Gu et al. 2020). High O_3 concentrations at the surface are usually accompanied by high temperature and low relative humidity (Li et al. 2021) because high temperatures and solar UV radiation usually significantly enhance the biological emissions of VOCs (Wang et al. 2018).

We utilize PI coefficients to quantify further the contribution of each driver to the ozone prediction. The findings align with the results from the ablation experiments (Fig. 4). Historical ozone concentration exhibits the highest contribution, followed by wind speed (u, v), temperature,

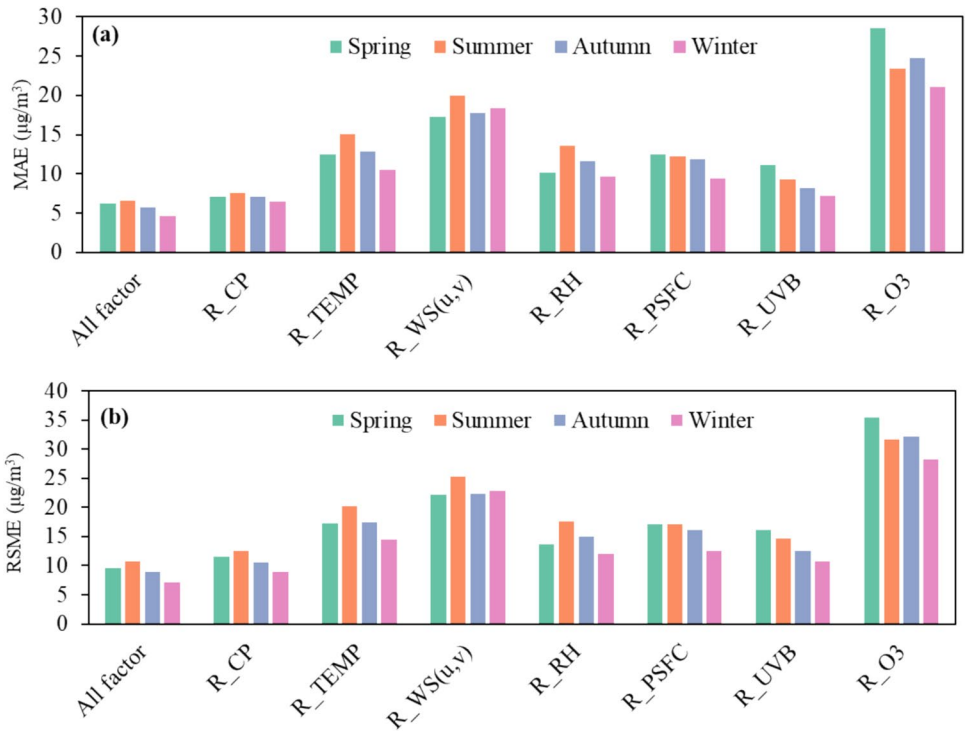

Fig. 3 The spatial-temporally averaged MAE and RMSE for the ablation experiments. The removed factors in different scenarios: All factors–nothing; R_CP–conventional pollutants; R_TEMP–temperature; R_WS(u,v)–wind speed(u,v); R_RH–relative humidity; R_PSFC–pressure; R_UVB–downward UV radiation at the surface; R_O_3–historical ozone

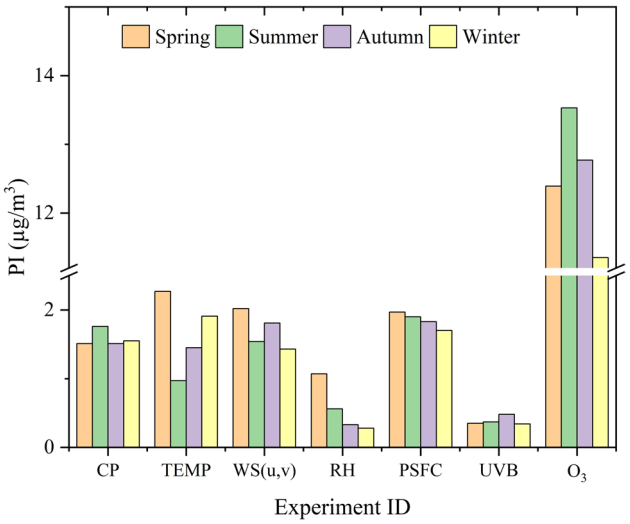

Fig. 4 The permutation importance for the multi factors in the MRD-O_3former

and pressure. The analysis of key driving factors indicates that historical ozone concentration and wind direction and speed have a greater impact on short-term ozone predictions at a regional scale. This is reasonable considering the longer atmospheric lifetime of ozone, allowing for its accumulation and long-distance transport in the atmosphere.

Application in the polluted small region

The results above demonstrate that our developed model can be applied to spatiotemporal ozone prediction at a national scale. To further validate the model's applicability, we utilized data from a polluted area within a smaller region, specifically the Beijing-Tianjin-Hebei (BTH) region. BTH, known for its high population density, has experienced elevated ozone concentrations in recent years. The summer mean MDA8-O_3 in the BTH region exhibited an increasing trend of 3.3 ppbv per year from 2013 to 2019 (Li et al. 2020).

The comparison results of the predictions (NMB and RMSE) are presented in Table 1. The results indicate that, compared to the predictions based on national-scale data, the simulated results based on the smaller region data showed improvement in the predictions for spring and summer, with NMB values changing from −2.67% and −5.87% to 0.96% and −5.83%, respectively. However, the predictions for autumn and winter deteriorated, with NMB values changing from 0.13% and −2.30% to 9.39% and 3.38%, respectively. There was a slight overestimation of ozone concentrations in autumn and winter, particularly in autumn, although the reasons for this overestimation are currently unclear. Overall, the BTH regional model's deviations are acceptable, with a maximum deviation of approximately 9.39%. Furthermore, the model adequately captures the spatial distribution of ozone concentrations in small areas and exhibits predictive capabilities. This finding strongly supports the implementation of more detailed environmental monitoring and management at smaller scales based on the prediction of MRD-O_3former.

Differential impact factors in urban–rural prediction

Past ozone predictions have often been based on analyses of urban monitoring stations, resulting in limited spatial distribution forecasts and less attention to ozone in rural areas. However, recent studies have found that rural residents are exposed to ambient ozone concentrations of 9.8 ±4.1 ppbv higher than their urban counterparts (Sun et al. 2023), highlighting the importance of focusing on rural areas. Unfortunately, rural areas often lack the capacity to establish monitoring stations, making ozone prediction in these regions even more crucial. Therefore, we conducted an analysis by isolating urban and rural areas using city-wide grid data from the Global Rural–Urban Mapping Project (GRUMP) (https://sedac.ciesin.columbia.edu/data/collection/grump-v1, last access: 12 April 2024). Urban areas were defined based on continuous night lighting units or buffer dwelling points with a population of over 5,000 people.

Figure 5 presents the PI coefficients for each driver in urban and rural areas. It indicates that, at the city scale, factors such as temperature, wind speed, and pressure have a minor contribution to ozone formation, while historical ozone levels, conventional pollutants, and solar UV radiation play a more significant role. Interestingly, during the summer, the impact of historical ozone levels on the prediction results is negative. This suggests that due to strong photochemical reactions, the next day's ozone concentration is primarily influenced by secondary formation and has little correlation with the ozone concentration of the previous day. In the rural environment, historical ozone levels play a significant role, which is reasonable (Zhu et al. 2020). With lower precursor concentrations, the next day's ozone concentration is largely determined by the ozone levels of the previous day, and secondary formation is relatively smaller. Additionally, factors such as wind speed, pressure, and temperature show a

Table 1 The NMB (RMSE) of modeled results by smaller and national-scale data in BTH

	Spring	Summer	Autumn	Winter
national-scale based	−2.67% (19.87)	−5.87% (26.24)	0.13% (14.83)	−2.30% (11.32)
Smaller region based	0.96% (21.79)	−5.83% (27.80)	9.39% (16.55)	3.38% (12.68)

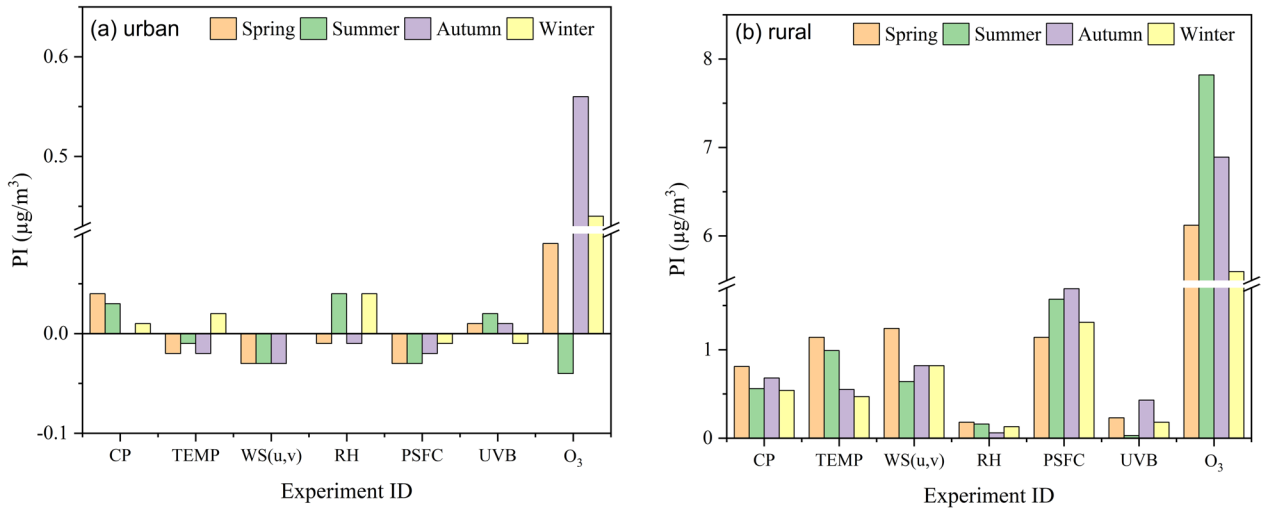

Fig. 5 The PI coefficients for each factor in urban (**a**) and rural (**b**) areas

more noticeable influence on ozone. These findings provide valuable insights into the mechanisms driving changes in ozone concentrations across different geographical contexts, highlighting the distinct differences in the driving factors for ozone prediction in urban and rural areas. Further detailed research should be conducted in the future to deepen our understanding of the differences between urban and rural areas.

Conclusion and atmospheric implication

In this study, we developed the MRD-O_3former model for short-term ozone prediction. The model exhibited excellent performance, with a high correlation coefficient (r^2) ranging from 0.85 to 0.90 and relatively low normalized mean biases (NMBs) between −15% and 15% at the national scale. Through multi-factor ablation experiments and PI analysis, we investigated the crucial factors for ozone prediction in different seasons and discovered that ozone formation is influenced by the complex interactions of multiple drivers rather than a single key factor. In most cases, historical ozone levels were found to be the key factor affecting ozone prediction for the following day, while meteorological factors such as wind speed and temperature also had a significant impact on ozone prediction.

We further validated the model's utility at the regional scale and found that the developed model demonstrated good applicability in the Beijing-Tianjin-Hebei region. It can be used for ozone pollution prediction and management at the regional or city scale. In the perturbation experiments conducted separately for urban and rural areas, we observed that the impact of meteorological factors was more prominent in rural regions compared to urban areas, while historical ozone levels had minimal influence on ozone pollution in urban areas. This result may be attributed to the fact that in urban areas, the ozone generated on the following day predominantly originates from secondary formation, whereas in rural areas, it is primarily influenced by the ozone concentration of the previous day (with relatively less secondary formation).

The findings of this study underscore the promising potential of deep learning techniques for interpretive spatio–temporal short-term predictions for surface ozone. It is important to note that, based on the hourly results, the model exhibits larger errors in simulating ozone levels during periods of intense photochemical activity, particularly during midday (Fig. S3). This is consistent with the finding that the simulation errors are greatest in summer compared to other seasons. These results suggest that the model's current input parameters may not fully capture the photochemical processes driving ozone formation, especially during midday. Additionally, given the intricate relationship between ozone precursors and meteorological variables, future research will focus on analyzing more detailed connections among various ozone drivers to enhance the accuracy of ozone predictions further. This deeper understanding will contribute to improved air quality management and the development of effective strategies for mitigating ozone pollution.

Supplementary Information The online version contains supplementary material available at https://doi.org/10.1007/s11869-025-01749-w.

Acknowledgements We are grateful for the comments of two anonymous reviewers.

Authors'contributions Canju Zheng: Formal analysis, writing-original draft. Hengqing Shen: Conceptualization, formal analysis, writing-review & editing. Jianan Sun: Writing-review & editing, investigation. Guangliang Liu: Supervision, conceptualization, writing-review

& editing. Haowei Cao: Investigation, data curation. Jie Zhang: Investigation. Xiang Gong: Data curation. Da Xu: Data curation.

Funding This study is financially supported by the Major Innovation Special Project for the Integration of Science, Education, Industry of Qilu University of Technology (Shandong Academy of Science) (No. 2023 JBZ02 and 2023HYZX01), Jinan Science and Technology Bureau (No. 202228034), Open Funds for Hubei Key Laboratory of Marine Geological Resources, China University of Geosciences (No. MGR202207), Key R&D Program of Shandong Province, China (No. 2022 CXGC020106) and the China Postdoctoral Science Foundation (No. 2021M691921).

Data availability The data supporting this study are available upon request from the corresponding author.

Declarations

Ethics approval and consent to participate Not applicable.

Consent for publication Not applicable.

Competing interests The authors have no financial or non-financial interests to disclose.

References

Chen Z, Li R, Chen D, Zhuang Y, Gao B, Yang L, Li M (2020) Understanding the causal influence of major meteorological factors on ground ozone concentrations across China. J Clean Prod 242:118498. https://doi.org/10.1016/j.jclepro.2019.118498

Cheng M, Fang F, Navon IM, Zheng J, Tang X, Zhu J, Pain C (2022) Spatio-temporal hourly and daily ozone forecasting in China using a hybrid machine learning model: autoencoder and generative adversarial networks. J Adv Model Earth Syst 14:e2021MS002806. https://doi.org/10.1029/2021MS002806

Ganji A, Minet L, Weichenthal S, Hatzopoulou M (2020) Predicting traffic-related air pollution using feature extraction from built environment images. Environ Sci Technol 54:10688–10699. https://doi.org/10.1021/acs.est.0c00412

Gao Z, Shi X, Wang H, Zhu Y, Wang Y, Li M, Yeung D-Y (2022a) Earthformer: exploring space-time transformers for earth system forecasting. Adv Neural Inf Process Syst 35:25390–25403

Gao Z, Shi X, Wang H, Zhu Y, Wang Y, Li M, Yeung D-Y (2022b) Earthformer: exploring space-time transformers for earth system forecasting. Adv Neural Inf Process Syst 35:25390–25403

Gong C, Liao H, Yue X, Ma Y, Lei Y (2021) Impacts of ozone-vegetation interactions on ozone pollution episodes in north China and the Yangtze river delta. Geophys Res Lett 48:e2021GL093814. https://doi.org/10.1029/2021GL093814

Gu Y, Li K, Xu J, Liao H, Zhou G (2020) Observed dependence of surface ozone on increasing temperature in Shanghai, China. Atmos Environ 221:117108. https://doi.org/10.1016/j.atmosenv.2019.117108

He C, Wu Q, Li B, Liu J, Gong X, Zhang L (2023) Surface ozone pollution in China: trends, exposure risks, and drivers. Front Public Health 11:1131753. https://doi.org/10.3389/fpubh.2023.1131753

Hong F, Ji C, Rao J, Chen C, Sun W (2023) Hourly ozone level prediction based on the characterization of its periodic behavior via deep learning. Process Saf Environ Prot 174:28–38. https://doi.org/10.1016/j.psep.2023.03.059

Huang F, Zhang Y, Zhang Ye, Shangguan W, Li Q, Li L, Jiang S (2023) Interpreting Conv-LSTM for spatio-temporal soil moisture prediction in China. Agriculture 13:971. https://doi.org/10.3390/agriculture13050971

Li S, Wang T, Huang X, Pu X, Li M, Chen P, Yang X-Q, Wang M (2018) Impact of east asian summer monsoon on surface ozone pattern in China. J Geophys Res Atmospheres 123:1401–1411. https://doi.org/10.1002/2017JD027190

Li K, Jacob DJ, Shen L, Lu X, De Smedt I, Liao H (2020) Increases in surface ozone pollution in China from 2013 to 2019: anthropogenic and meteorological influences. Atmospheric Chem Phys 20:11423–11433. https://doi.org/10.5194/acp-20-11423-2020

Li M, Yu S, Chen X, Li Z, Zhang Y, Wang L, Liu W, Li P, Lichtfouse E, Rosenfeld D, Seinfeld JH (2021) Large scale control of surface ozone by relative humidity observed during warm seasons in China. Environ Chem Lett 19:3981–3989. https://doi.org/10.1007/s10311-021-01265-0

Liang Y, Xia Y, Ke S, Wang Y, Wen Q, Zhang J, Zheng Y, Zimmermann R (2023) AirFormer: predicting nationwide air quality in China with transformers. Proc AAAI Conf Artif Intell 37:14329–14337. https://doi.org/10.1609/aaai.v37i12.26676

Liu Y, Geng G, Cheng J, Liu Y, Xiao Q, Liu L, Shi Q, Tong D, He K, Zhang Q (2023) Drivers of increasing ozone during the two phases of clean air actions in China 2013–2020. Environ Sci Technol 57:8954–8964. https://doi.org/10.1021/acs.est.3c00054

Mu X, Wang S, Jiang P, Wang B, Wu Y, Zhu L (2023a) Full-coverage spatiotemporal estimation of surface ozone over China based on a high-efficiency deep learning model. Int J Appl Earth Obs Geoinformation 118:103284. https://doi.org/10.1016/j.jag.2023.103284

Mu X, Wang S, Jiang P, Wu Y (2023b) Estimation of surface ozone concentration over Jiangsu province using a high-performance deep learning model. J Environ Sci 132:122–133. https://doi.org/10.1016/j.jes.2022.09.032

Pak U, Kim C, Ryu U, Sok K, Pak S (2018) A hybrid model based on convolutional neural networks and long short-term memory for ozone concentration prediction. Air Qual Atmos Health 11:883–895. https://doi.org/10.1007/s11869-018-0585-1

Pan Q, Harrou F, Sun Y (2023) A comparison of machine learning methods for ozone pollution prediction. J Big Data 10:63. https://doi.org/10.1186/s40537-023-00748-x

Sayeed A, Eslami E, Lops Y, Choi Y (2022) CMAQ-CNN: a new-generation of post-processing techniques for chemical transport models using deep neural networks. Atmos Environ 273:118961. https://doi.org/10.1016/j.atmosenv.2022.118961

Shu L, Zhu L, Bak J, Zoogman P, Han H, Liu S, Li X, Sun S, Li J, Chen Y, Pu D, Zuo X, Fu W, Yang X, Fu T-M (2023) Improving ozone simulations in Asia via multisource data assimilation: results from an observing system simulation experiment with GEMS geostationary satellite observations. Atmospheric Chem Phys 23:3731–3748. https://doi.org/10.5194/acp-23-3731-2023

Sun HZ, Zhao J, Liu X, Qiu M, Shen H, Guillas S, Giorio C, Staniaszek Z, Yu P, Wan MWL, Chim MM, Van Daalen KR, Li Y, Liu Z, Xia M, Ke S, Zhao H, Wang H, He K, Liu H, Guo Y, Archibald AT (2023) Antagonism between ambient ozone increase and urbanization-oriented population migration on Chinese cardiopulmonary mortality. The Innovation 4:100517. https://doi.org/10.1016/j.xinn.2023.100517

Wang T, Xue L, Brimblecombe P, Lam YF, Li L, Zhang L (2017) Ozone pollution in China: a review of concentrations, meteorological influences, chemical precursors, and effects. Sci Total Environ 575:1582–1596. https://doi.org/10.1016/j.scitotenv.2016.10.081

Wang H, Wu Q, Liu H, Wang Y, Cheng H, Wang R, Wang L, Xiao H, Yang X (2018) Sensitivity of biogenic volatile organic compound emissions to leaf area index and land cover in Beijing. Atmos Chem Phys 18:9583–9596. https://doi.org/10.5194/acp-18-9583-2018

Wen Y, Zhou Z, Zhang S, Wallington TJ, Shen W, Tan Q, Deng Y, Wu Y (2022) Urban-rural disparities in air quality responses to traffic changes in a megacity of China revealed using machine learning. Environ Sci Technol Lett 9:592–598. https://doi.org/10.1021/acs.estlett.2c00246

Wu C, He H, Song R, Zhu X, Peng Z, Fu Q, Pan J (2023) A hybrid deep learning model for regional O3 and NO2 concentrations prediction based on spatiotemporal dependencies in air quality monitoring network. Environ Pollut 320:121075. https://doi.org/10.1016/j.envpol.2023.121075

Xiong K, Xie X, Mao J, Wang K, Huang L, Li J, Hu J (2023) Improving the accuracy of O3 prediction from a chemical transport model with a random forest model in the Yangtze River Delta region, China. Environ Pollut 319:120926. https://doi.org/10.1016/j.envpol.2022.120926

Xu H, Yu H, Xu B, Wang Z, Wang F, Wei Y, Liang W, Liu J, Liang D, Feng Y, Shi G (2023) Machine learning coupled structure mining method visualizes the impact of multiple drivers on ambient ozone. Commun Earth Environ 4:265. https://doi.org/10.1038/s43247-023-00932-0

Yang J, Zhao Y (2023) Performance and application of air quality models on ozone simulation in China – A review. Atmos Environ 293:119446. https://doi.org/10.1016/j.atmosenv.2022.119446

Yang J, Liu J, Han S, Yao Q, Cai Z (2019) Study of the meteorological influence on ozone in urban areas and their use in assessing ozone trends in all seasons from 2009 to 2015 in Tianjin, China. Meteorol Atmos Phys 131:1661–1675. https://doi.org/10.1007/s00703-019-00664-x

Yin X, Rupakheti D, Zhang G, Luo J, Kang S, de Foy B, Yang J, Ji Z, Cong Z, Rupakheti M, Li P, Hu Y, Zhang Q (2023) Surface ozone over the tibetan plateau controlled by stratospheric intrusion. Atmos Chem Phys 23:10137–10143. https://doi.org/10.5194/acp-23-10137-2023

Yu R, Lin Y, Zou J, Dan Y, Cheng C (2021) Review on atmospheric ozone pollution in china: formation, spatiotemporal distribution, precursors and affecting factors. Atmosphere 12(12):1675

Zhang Z, Zhang S, Chen C, Yuan J (2024) A systematic survey of air quality prediction based on deep learning. Alex Eng J 93:128–141. https://doi.org/10.1016/j.aej.2024.03.031

Zhu X, Ma Z, Qiu Y, Liu H, Liu Q, Yin X (2020) An evaluation of the interaction of morning residual layer ozone and mixing layer ozone in rural areas of the North China plain. Atmospheric Res 236:104788. https://doi.org/10.1016/j.atmosres.2019.104788